

## Hydrodynamic modification of an expanding plasma by laser radiation

Zhi-zhan Xu, Wei Yu, and Wen-qi Zhang

Shanghai Institute of Optics and Fine Mechanics, Academia Sinica, P. O. Box 8211,  
Shanghai, People's Republic of China

(Received 9 October 1984)

The hydrodynamic modification of an expanding plasma by the ponderomotive force of the laser radiation is calculated without introducing the assumption of the density profile being locally linear from the sonic point to the critical density. Intensity dependence of various parameters which characterize the density profile modification are presented. Our results can reflect the density jump occurring in the critical region more completely and accurately. In addition, the field structure and the density profile for all regions of coronal plasma are also studied.

### I. INTRODUCTION

Experiments<sup>1</sup> and particle simulations<sup>2,3</sup> have shown that, when the incident laser radiation is strong enough, the ponderomotive force of the laser radiation can dramatically modify the hydrodynamic behavior of the plasma in the critical density region: The density profile close to the critical point is locally steepened, while connecting regions of nearly uniform density are formed above and below. Since the hydrodynamic modification in the critical density region plays an important role in laser light absorption and scattering processes, it has become a topic of current interest in laser plasma interaction research.

In this paper, the hydrodynamic modification of a freely expanding plasma by the ponderomotive force of a normally incident laser light or an obliquely incident, *s*-polarized laser light will be studied. In former works, Lee *et al.*<sup>4</sup> calculated the lower- and upper-shelf densities and the flow speed as functions of incident power, but their calculation did not characterize the steepened profile between the two density shelves. Recently, by approximating the plasma density profile as locally linear from the density at the sonic point ( $n_s$ ) to the critical density ( $n_{cr}$ ), Kruer and Estabrook<sup>5</sup> further investigated the profile steepening, and determined the scale length for that steepened linear layer. In the following analysis we will present the intensity dependence of a series of parameters by removing the locally linear assumption. With these parameters, we cannot only characterize the hydrodynamic modification in the critical region more accurately and completely, but also determine the electric-field structure and the density profile in the coronal region of the expanding plasma self-consistently.

### II. THEORY

We consider a collisionless, inhomogeneous plasma with plasma density  $n = n(x)$  and plasma flow speed  $v = v(x)$ . In the frame moving with the density jump, the hydrodynamic behavior of plasma in the critical region is governed by following steady-state equations:<sup>4,5</sup>

$$\frac{\partial}{\partial \xi} (NV) = 0, \tag{1}$$

$$V \frac{\partial V}{\partial \xi} = \frac{1}{4} \frac{\partial}{\partial \xi} A^2 - \frac{1}{N} \frac{\partial N}{\partial \xi}, \tag{2}$$

$$\frac{\partial^2 A}{\partial \xi^2} + (1-N)A = 0, \tag{3}$$

where  $\xi = x\omega/c$ ,  $V = v/c_s$ ,  $N = n/n_{cr}$ ,  $A = eE/m\omega v_e$ ,  $c_s = (ZT_e/m_i)^{1/2}$  is the ion sound speed,  $v_e = (T_e/m)^{1/2}$  is the electron thermal speed, and  $e$ ,  $m$ ,  $T_e$ ,  $m_i$ ,  $Z$ ,  $\omega$ , and  $E$  are the electron charge, electron mass, electron temperature, ion mass, ion charge number, laser frequency, and electric field, respectively.

Equations (1) and (2) yield

$$\frac{\partial A^2}{\partial \xi} = -4 \left( V - \frac{1}{V} \right) \frac{\partial V}{\partial \xi}. \tag{4}$$

At the sonic point where  $V=1$ ,  $A_s$  and  $(\partial V/\partial \xi)_s$  remain finite, which requires  $(\partial A/\partial \xi)_s = 0$ , so the sonic point must be at the maximum of the electric field.<sup>5</sup> From Eqs. (1) and (4), we have<sup>4,5</sup>

$$NV = N_s, \tag{5}$$

$$2(V^2 - \ln V^2 - 1) = A_s^2 - A^2. \tag{6}$$

Multiplying Eq. (3) by  $A' = \partial A/\partial \xi$ , and substituting Eq. (4) into it, we obtain

$$\begin{aligned} \frac{\partial}{\partial \xi} (A')^2 + (1-N) \frac{\partial A^2}{\partial \xi} \\ = \frac{\partial}{\partial \xi} (A')^2 + 4 \left( 1 - \frac{N_s}{V} \right) \left( \frac{1}{V} - V \right) \frac{\partial V}{\partial \xi} = 0. \end{aligned}$$

The equation can be integrated to yield

$$(A')^2 + A^2 - A_s^2 + 4N_s \left( V + \frac{1}{V} - 2 \right) = 0. \tag{7}$$

Rewrite Eq. (4) in the form

$$(A')^2 = 4 \frac{(V^2 - 1)^2}{A^2 V^2} \left( \frac{\partial V}{\partial \xi} \right)^2.$$

Substituting it into Eq. (7) yields

$$\begin{aligned} \frac{\partial V}{\partial \xi} = \frac{V}{|V^2 - 1|} \left[ V^2 - \ln V^2 - 1 - \frac{2N_s}{V} (V-1)^2 \right]^{1/2} \\ \times \left[ \frac{A_s^2}{2} - (V^2 - \ln V^2 - 1) \right]^{1/2}. \end{aligned} \tag{8}$$

Since the electric field at the upper-density shelf is evanes-

cent,  $A$  and  $\partial A/\partial \xi$  both tend to zero, Eqs. (6) and (8) yield

$$A_s^2 = 2(V_2^2 - \ln V_2^2 - 1), \quad (9)$$

$$N_s = \frac{V_2 A_s^2}{4(V_2 - 1)^2}, \quad (10)$$

where  $N_2$  and  $V_2$  are the upper-shelf density and the upper-shelf flow speed. At the lower-density shelf where  $A = 0$  but  $\partial A/\partial \xi \neq 0$ , Eq. (6) yields

$$V_2^2 = \frac{2 \ln \beta}{\beta^2 - 1}, \quad (11)$$

where  $\beta = V_1/V_2 = N_2/N_1$ ;  $N_1$  and  $V_1$  are the lower-shelf density and the lower-shelf flow speed.

The steepening of the plasma density profile is usually characterized by the local scale length

$$L(x) = |n(x)/(dn/dx)| = (1/k_0) |N/(dN/d\xi)|.$$

Since  $(dN/d\xi) = -(N/V)(dV/d\xi)$ , the local scale length inside the critical region (except at the sonic point) is readily determined by using Eq. (8). For example, at the critical point where  $N = 1$ ,  $V = N_s$ ,

$$k_0 L_{cr} = \sqrt{2(1 - N_s^2)[4N_s - N_s^2 - \ln N_s^2 - 3]}^{-1/2} \times [A_s^2 - 2(N_s^2 - \ln N_s^2 - 1)]^{-1/2}. \quad (12)$$

The scale length at the sonic point can be determined in another way. Differentiating Eq. (4) with respect to  $\xi$  and substituting Eq. (3) into it, we get

$$\begin{aligned} \left(1 + \frac{1}{V^2}\right) \left(\frac{\partial V}{\partial \xi}\right)^2 + \left(V - \frac{1}{V}\right) \frac{\partial^2 V}{\partial \xi^2} &= -\frac{1}{2} \left[ \left(\frac{\partial A}{\partial \xi}\right)^2 + A \frac{\partial^2 A}{\partial \xi^2} \right] \\ &= -\frac{1}{2} \left[ \left(\frac{\partial A}{\partial \xi}\right)^2 - (1 - N)A^2 \right]. \end{aligned}$$

At the sonic point where  $V = 1$ ,  $N = N_s$ ,  $A = A_s$ ,  $(\partial A/\partial \xi) = 0$ , we have

$$k_0 L_s = 2/A_s \sqrt{1 - N_s}. \quad (13)$$

Equations (9)–(13) have established the interdependent relations between the parameters characterizing the profile modification. It must be indicated that the above calculations are valid only in the critical region. In the underdense region, however, the calculations will lead to the obviously unreasonable conclusions that  $A(\xi)$  oscillates between  $A_1$  and  $A_s$ , while  $N(\xi)$  oscillates between  $N_1$  and  $N_s$ .<sup>4,5</sup> This is because the derivation of Eqs. (6) and (7) requires  $A$  and  $A'$  to be single-valued functions of variable  $V$ . Moreover, in the underdense region, the plasma is expanding to the vacuum, and is by no means regarded as in steady state even in the frame moving with the density jump; as a result, Eqs. (1) and (2) are no longer valid either. However, since the ponderomotive modification occurs mainly in the critical region (i.e., near the reflection point of the light wave where its momentum is locally deposited), while the underdense plasma is scarcely affected by the ponderomotive force, the plasma density profile in the underdense region is well described by the self-similar solution of the non-steady-state hydrodynamic equations<sup>3</sup>

$$N(\xi) = N_1 \exp[(\xi_1 - \xi)/k_0 c_s t], \quad (14)$$

where  $\xi_1 = k_0 x_1$ ,  $x_1$  is the coordinate of the lower-density

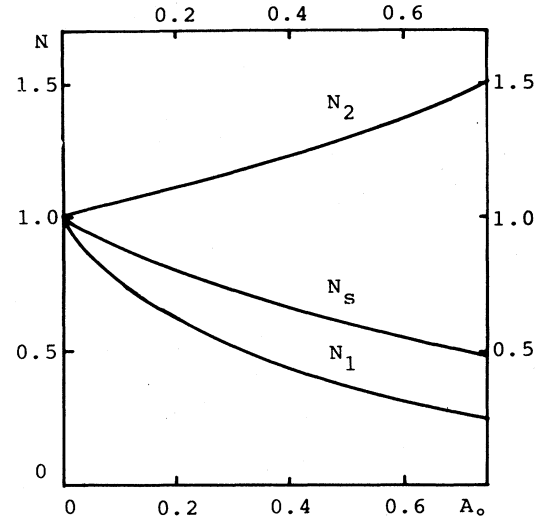


FIG. 1. The  $A_0$  dependence of the upper-shelf density, the lower-shelf density, and the plasma density at the sonic point.

shelf. The scale length of the underdense plasma  $L(x) = c_s t \sim c_s \tau$ , where  $\tau$  is the pulse width of laser. Since  $L$  is much larger than the wavelength of laser in vacuum, the electric field structure in the underdense plasma can be derived by using the WKB method:

$$A(\xi) = \frac{2A_0}{4\sqrt{\epsilon}} \sin \left[ -k_0 L \left( 2\sqrt{\epsilon} + \ln \frac{1 - \sqrt{\epsilon}}{1 + \sqrt{\epsilon}} + C \right) \right], \quad (15)$$

where

$$\epsilon = 1 - N, \quad C = -2\sqrt{\epsilon_1} - \ln[(1 - \sqrt{\epsilon_1})/(1 + \sqrt{\epsilon_1})],$$

$$\epsilon_1 = 1 - N_1, \quad A_0 = eE_0/m\omega v_e,$$

and  $E_0$  is the electric field of laser in vacuum. According to

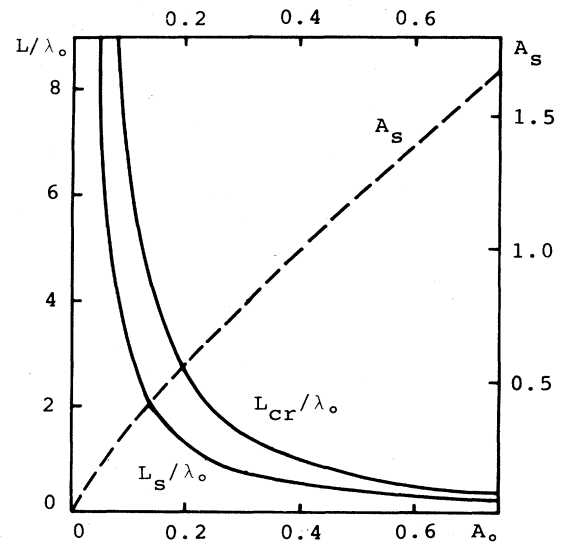


FIG. 2. The  $A_0$  dependence of the local scale length at the sonic point and the critical point (—), and the  $A_0$  dependence of the electric field at the sonic point (---).

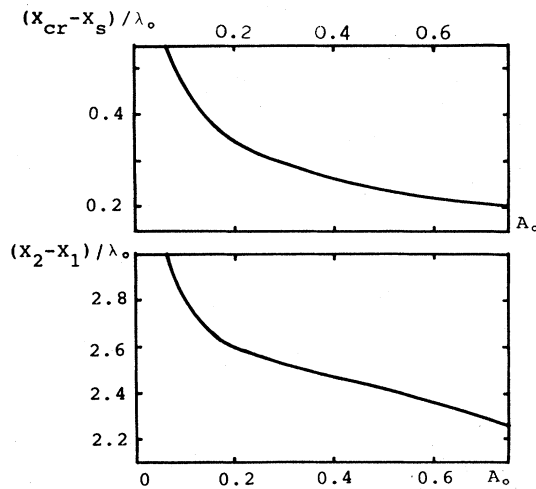


FIG. 3. The  $A_0$  dependence of the distance between the sonic point and the critical point, and the distance between the upper- and lower-density shelves.

Eq. (15), the derivative of  $A(\xi)$  at the lower-density shelf will be

$$A'(\xi_1) = 2A_0 \sqrt[4]{1 - N_1}, \quad (16)$$

while according to Eq. (7), it will be

$$A'(\xi_1) = [A_s^2 - 4N_s(V_1 + 1/V_1 - 2)]^{1/2}. \quad (17)$$

From these two equations, we have

$$A_0^2 = (N_2 - N_1)(N_1 N_2 - N_s^2) / N_1 N_2 \sqrt{1 - N_1}. \quad (18)$$

### III. CONCLUSIONS

Equation (18), together with Eqs. (9)–(13), can completely determine the  $A_0$  dependence of all the corresponding parameters. Figures 1 and 2 show (1) for any specified value of  $A_0$ , we always have  $N_2 > N_{cr} > N_s > N_1$  and (2) when  $A_0 > 0.5$ ,  $L_s$  and  $L_{cr}$  are about the same value, but when  $A_0 < 0.5$ , their difference is remarkable. Such a situation is by no means distinguished by using locally linear assumption. The curves in Figs. 1 and 2 are well approximat-

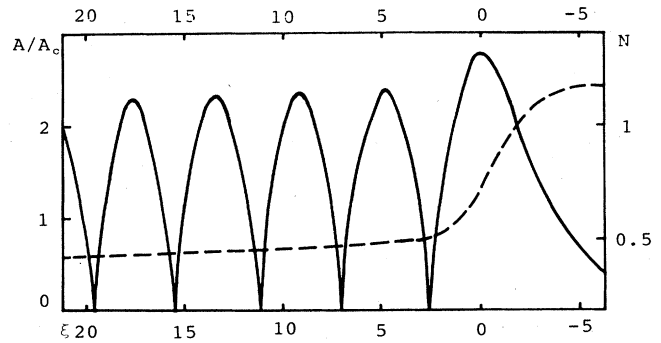


FIG. 4. The electric-field structure (—) and the plasma density profile (---) in coronal plasma, where  $A_0 = 0.325$ ,  $k_0 L = 100$ .

ed by functions in the form  $f(x) = Ax^b$ , and thus yield the following scale laws:

$$\begin{aligned} A_s &= 2.1A_0^{0.82}, & N_s &= 1 - 0.66A_0^{0.8}, \\ N_1 &= 1 - 0.97A_0^{0.64}, & N_2 &= 1 + 0.59A_0^{0.98}, \\ L_s/\lambda_0 &= 0.19A_0^{-1.22}, & L_{cr}/\lambda_0 &= 0.27A_0^{-1.37}. \end{aligned} \quad (19)$$

Integrating Eq. (8) with respect to  $V$ , and taking  $V_s$  as the lower integral limit, and  $V_2$ ,  $V_1$ ,  $V_{cr}$  as the upper integral limits, respectively, we determine the  $A_0$  dependence of coordinate  $x_2$ ,  $x_1$ , and  $x_{cr}$ . In Fig. 3, the distance between upper- and lower-density shelves, and the distance between sonic point and critical point are presented. The former can be regarded as the width of the critical region, while the latter characterizes the area where the density gradient is obviously steepened.

The electric-field structure and the density profile in coronal plasma are described by Eqs. (5), (6), (8), (14), and (15). From Fig. 4, it can be seen that our calculations are in good agreement with experiment and particle simulations.<sup>1,2,6</sup>

When an  $s$ -polarized light is obliquely incident, the hydrodynamic behavior of plasma near the reflection point (where  $n = n_{cr} \cos^2 \theta_0$ ,  $\theta_0$  is the angle of incidence) is still governed by Eqs. (1)–(3) only if we define  $N = n/n_{cr} \cos^2 \theta_0$ ,  $\xi = k_0 x \cos \theta_0$ . As a result, it is convenient for the analysis we present above to be expanded to the  $s$ -polarized, obliquely incident case.

<sup>1</sup>A. Y. Wang, in *Laser Interaction and Related Plasma Phenomena*, edited by H. J. Schwartz and H. Hora (Plenum, New York, 1977), Vol. 4B, p. 657.

<sup>2</sup>D. W. Forslund, J. M. Kindel, and E. L. Lindman, *Phys. Rev. Lett.* **36**, 35 (1976).

<sup>3</sup>R. D. Jones *et al.*, *Phys. Fluids* **24**, 310 (1981).

<sup>4</sup>K. Lee *et al.*, *Phys. Fluids* **20**, 51 (1977).

<sup>5</sup>W. L. Kruer and K. G. Estabrook, *Phys. Fluids* **26**, 1888 (1983).

<sup>6</sup>W. C. Mead *et al.*, *Phys. Fluids* **26**, 2316 (1983).